ISSN 1063-7745, Crystallography Reports, 2008, Vol. 53, No. 2, pp. 177–182. © Pleiades Publishing, Inc., 2008.
Original Russian Text © V.G. Kohn, 2008, published in Kristallografiya, 2008, Vol. 53, No. 2, pp. 203–209.

DIFFRACTION AND SCATTERING OF IONIZING RADIATIONS

Trajectory Method in the Theory of Laue Diffraction of X rays in Crystals: II. Effect of Total Reflection at Bending Deformation

V. G. Kohn

Russian Research Centre Kurchatov Institute, pl. Akademika Kurchatova 1, Moscow, 123182 Russia
e-mail: kohnvict@yandex.ru

Received June 6, 2007

Abstract—The effect of total reflection (switching) of a spherical X-ray wave in the case of Laue diffraction in a crystal with bending deformation is analyzed by the trajectory method. Qualitative analytical description and computation of the spatial structure of the reflected beam for large and small distances between the spherical-wave source and the crystal are performed. The mechanism of much more efficient reflection of an X-ray beam by a deformed crystal in comparison with a perfect crystal is clearly demonstrated. It is also shown that the trajectory method is very convenient for description of the total reflection phenomenon.

PACS numbers: 61.10.Nz

DOI: 10.1134/S1063774508020028

INTRODUCTION

It is well known that a thick single-crystal plate poorly scatters X rays for the following reason: a crystal is homogeneous if its electron density is averaged over the lattice constant; therefore, the crystal can scatter only in the forward direction. If the density is not averaged, additional scattering at the double Bragg angle occurs at a certain crystal orientation; this scattering is limited to a very narrow angular region, whose width is determined by the diffraction parameter $\chi_{rh} \sim 10^{-5}$, i.e., the Fourier component of the polarizability at the reciprocal lattice vector. It is also known that the integrated Bragg reflection intensity increases if a crystal contains defects or when its lattice is deformed. Hence, deformed crystals are interesting not only for diagnostics of their structure but also as objects having enhanced reflecting ability. A general formulation of the trajectory method in the theory of X-ray diffraction in the Laue geometry, where the reflected beam emerges from the opposite crystal face, was given in [1]. This method makes it possible to easily study the diffraction of a spherical wave in a crystal with slowly varying deformation.

In this study, the trajectory method is used for detailed analysis of the total reflection phenomenon in the case of Laue diffraction in a crystal with bending deformation. This effect, first observed in [2], was referred to as beam switching from the transmission to the reflection direction. The case in point is that the integrated intensity of a beam of finite width (for example, limited by a slit) increases and reaches a maximum with an increase in the strain of special kind. Simultaneously, the intensity of the transmitted beam tends toward zero, as a result of which the reflection can be considered as complete. A large number of experimental and theoretical studies were devoted to the switching effect; a brief review can be found in [3].

However, the trajectory method has not been used, although this method gives a simple qualitative description of the effect and significantly reduces the computation time. Analytical analysis is given in the next section. The essence of the effect is that the diffraction conditions are not satisfied near the input crystal surface, and X rays first propagate in the incident beam direction. As a result of the change in the crystal deformation, the Bragg condition becomes satisfied at a certain depth, and rays are effectively reflected. Then, the Bragg condition is violated again and the rays propagate in the reflection direction until they reach the crystal boundary. Independent of the angle at which a ray enters a crystal, it exits in the reflection direction. Its initial direction determines only the depth in the crystal at which reflection occurs. At the same time, a perfect crystal deviates rays at the input surface, after which they do not change their direction since the Bragg condition remains the same throughout the crystal. Therefore, only the rays entering the crystal in the appropriate direction are reflected.

Numerical calculations were performed for two limiting cases of large (40 m) and small (50 cm) distances between the spherical-wave source and the crystal. In the first case, the spatial structure of the reflected beam almost reproduces the angular dependence of reflection in the case of plane-wave diffraction. The second case is similar to the problem of diffraction of a spherical wave in the Kato formulation [4, 5], where the source is placed on the crystal surface. In both cases, an increase in deformation leads to complete reflection of a beam of

limited width, although with a certain loss of intensity for absorption in the crystal.

ANALYTICAL ANALYSIS

The general formulation of the trajectory method was given in [1]—the first part of this investigation. Below, the formulas of the first part are referred to with indication of the Roman numeral I before the number. The basic concepts of the theory are as follows. The variable scalar amplitudes of the electric field of the transmitted ($E_0(x, z)$) and diffracted ($E_h(x, z)$) waves in a crystal, corresponding to one of the two possible polarization states, are investigated. The coordinate axes x and z lie in the scattering plane and are oriented, respectively, parallel and perpendicularly to the crystal surface; the x axis is directed toward the incident beam and the z coordinate is zero at the input crystal surface. These amplitudes in a deformed crystal satisfy the Takagi equation (I,2) with a variable parameter of deviation from the Bragg condition.

We consider the case where the strain only slightly changes at a distance of about the extinction length. In this case, the solutions to the equations are sought in the form of two independent Bloch waves in the eikonal approximation; i.e., the amplitude of each Bloch wave has the form $E_0 = BE_0''\exp(i\Phi)$ and $E_h = BFE_h''\exp(i\Phi)$. Here, $B = \exp(ic_0[s_0 + s_h])$, $c_0 = K\chi_0/2$, and $K = 2\pi/\lambda$ (λ is the X-ray wavelength and χ_0 is the average complex crystal polarizability, equal to its zero Fourier component). The oblique coordinates s_0 and s_h along the beam direction are linked to the Cartesian coordinates x and z by the following relations: $x = s_0\sin\theta_0 - s_h\sin\theta_h$ and $z = s_0\cos\theta_0 + s_h\cos\theta_h$, where θ_0 and θ_h are, respectively, the angles made by the vectors of the incident and diffracted waves with the internal normal to the crystal surface. Obviously, $\theta_0 + \theta_h = 2\theta_B$, where θ_B is the Bragg angle. In the case of symmetric diffraction, $\theta_0 = \theta_h = \theta_B$. The factor $F = \exp(-i\mathbf{h}[\mathbf{u}(\mathbf{r}) + \mathbf{u}_0])$, where $\mathbf{h}$ is the diffraction vector, the function $\mathbf{u}(\mathbf{r})$ describes the field of strain-induced atomic displacements, and $\mathbf{u}_0$ takes into account the choice of the reference point in the unit cell of the crystal (details in [1]).

Substituting the solution, we obtain two equations: one for the phase Φ (I,6) and the other for the amplitude E_0'' (I,17). The amplitude ratio $R = E_h''/E_0''$ is completely determined by the phase Φ. The equation for the phase Φ is solved by the trajectory method. Trajectories link each point on the input crystal surface with each point on the output surface. The initial amplitude E_0'' at each point on the input surface is found from expansion of the incident wave amplitude in two Bloch waves, with regard to validity of the local Bragg condition.

Concerning the equation, it can be solved analytically on a trajectory. The field amplitudes at the end of a trajectory are related to the incident wave amplitude E_{0i}'' at the beginning of the trajectory by formulas (I,24), which are given below in the explicit form

$$E_{0k}'' = \frac{1}{2}E_{0i}''(1 + V_0^{(k)})^{1/2}(1 + V_M^{(k)})^{1/2},$$
$$E_{hk}'' = \pm\frac{1}{2}E_{0i}''(1 + V_0^{(k)})^{1/2}(1 - V_M^{(k)})^{1/2}. \quad (1)$$

Here, the index $k = 1, 2$ enumerates Bloch waves with different refractive indices and absorption coefficients. The first wave ($k = 1$) is strongly absorbed, whereas the second wave ($k = 2$) is weakly absorbed. The parameter

$$V^{(k)} = \frac{dX}{dZ} = \pm\frac{y}{(1 + y^2)^{1/2}} \quad (2)$$

has the meaning of the rate of trajectory deviation from the Z axis. The upper sign corresponds to the first wave. The same parameter determines the direction of the energy flux in the crystal, since the energy flux in each Bloch wave propagates along trajectories. The coordinates $X = s_0 - s_h$ and $Z = s_0 + s_h$ are counted in the opposite direction and perpendicularly to the diffraction vector. In the case of symmetric diffraction, their relationship with the coordinates x and z, which were introduced above, has a simple form: $x = X\sin\theta_B$ and $z = Z\cos\theta_B$.

The parameter y plays a key role in the theory, since it corresponds to the dimensionless local parameter of deviation from the Bragg condition. The subscripts 0 and M on the velocity in formula (1) indicate that the values are taken at the beginning and end of a trajectory, i.e., on the input and output crystal surfaces. The equation for the parameter y takes into account the lattice strains in the crystal bulk. It can be written in the symmetric form

$$\frac{dy}{dZ} = \frac{1}{2c}\frac{\partial^2}{\partial s_0\partial s_h}(\mathbf{hu}(\mathbf{r})). \quad (3)$$

Here, $c = KC|\chi_{rh}|/2$, where C is the polarization factor (it is equal to 1 for σ polarization and $\cos(2\theta_B)$ for π polarization) and χ_{rh} is the Fourier component at the diffraction vector, taken from the real part of the crystal polarizability. The function on the right-hand side of the equation is taken on the calculated trajectory.

Equation (3) is solved with regard to boundary condition (I,18), which can be written in a more detailed form:

$$y_0 = \frac{1}{c}\left(\frac{\partial\Phi_0}{\partial X}\right)_{X_0} + \frac{\sin(2\theta_B)}{c}\Delta\theta + \frac{1}{2c}\frac{\partial}{\partial s_h}(\mathbf{hu}(\mathbf{r})). \quad (4)$$

Here, all variables are taken at the beginning of the trajectory, i.e., at the point X_0 on the input crystal surface ($Z = 0$); the angle $\Delta\theta$ takes into account the possible rotation of the crystal with respect to the optical axis; and the phase Φ_0 corresponds to the wave incident on

the crystal and is the initial value for the phase Φ, introduced above.

Equations (3) and (4) indicate that diffraction of an X-ray wave depends only on the component of the atomic displacement vector along the diffraction vector. In the symmetric case, this component is u_x. In this paper, we will consider bending deformation, i.e., assume that u_x depends only on z. In this case, we have total reflection of a plane wave in a wide angular range. Accordingly, total reflection of a spherical wave is implemented in the wide part of its front near the Bragg direction.

The trajectory method gives a very simple qualitative explanation of the total reflection phenomenon in the case of elastic bending of atomic planes. The simplest strain of such type arises upon heating of a lateral crystal face from the side of the reflected beam ([3] and a reference therein). It can be shown that in this case the strain at some distance from the lateral face is approximately described as the bending of atomic planes according to the parabolic law

$$u_x = -\frac{(z - t/2)^2}{2R}, \quad (5)$$

where t is the crystal thickness and R is the bending radius. In this formula, the term linear in x, which leads to a change in the interplanar spacing, is disregarded since it can easily be compensated for by appropriate choice of the Bragg angle. The formula is written in such a form that the displacement is counted from its value in the middle plane of the crystal. The constant term in the displacement is equivalent to the shift of a crystal as a whole and is also omitted. The displacement on the upper and lower faces is minimum since these faces are colder than the crystal bulk due to their contact with air.

Let the optical axis for the incident radiation be chosen in such a way that the Bragg condition is satisfied in the middle plane of the sample. We will consider a simple case where a plane wave is incident on a crystal along the optical axis. Then, only the second and third terms are nonzero in formula (4), and we have the following initial value of the parameter of deviation from the Bragg condition: $y_0 = y_c - Dt$, where $y_c = (\sin 2\theta_B/c)\Delta\theta$ and $D = \sin 2\theta_B/(2C|\chi_{rh}|R)$. Further evolution of this parameter is determined by Eq. (3), in which the right-hand side is constant; hence, the solution can be directly written in the form $y(z) = y_0 + 2Dz = y_c + 2D(z - t/2)$. To calculate the amplitudes, it is important to know only the value at the end of the trajectory, i.e., $y_M = y(t) = y_c + Dt$. Thus, the parameter y has different signs at different crystal faces if $|y_c| < Dt$. Since the rate of trajectory deviation is independent of x, all beam trajectories are parallel to each other (as in a plane wave) but are bent according to some law. At the exact Bragg position of the crystal and a large radius of curvature R, when $|y| \ll 1$, trajectories are described by the formula $x \approx x_0 \pm D\tan\theta_B z(z - t)$, i.e., are close to parabolas. However, with a decrease in R, the trajectory will have a parabolic portion only at some depth in the crystal; before and after this portion, trajectories are parallel, respectively, to the directions of the incident and reflected beams for the second Bloch wave and vice versa for the first wave.

It is also easy to calculate the field amplitudes according to (1). They have the simplest form for the Bragg position of the crystal ($y_c = 0$), specifically,

$$E''_{0k} = \frac{1}{2}E''_{0i}(1 - a^2)^{1/2}, \quad E''_{hk} = \pm\frac{1}{2}E''_{0i}(1 \mp a), \quad (6)$$

where $a = Dt/(1 + (Dt)^2)^{-1/2}$. It follows from formula (6) that, in the absence of strain, the amplitudes of both fields are equal in modulus. However, with an increase in strain, this equality is violated. In this case, the transmitted wave amplitude similarly decreases for each Bloch wave. The modulus of the reflected wave amplitude for the first Bloch wave decreases even faster; however, for the second (i.e., weakly absorbed) wave, the amplitude modulus, vice versa, increases. With an increase in strain, when $Dt > 1$, saturation occurs, at which the incident beam intensity tends toward zero at the crystal output, and the reflected beam intensity approaches a maximum, which is determined with allowance for the absorption loss. It is of interest that, for low strains, the effect relatively weakly depends on absorption, since specifically the weakly absorbed Bloch wave is reflected. The amplitudes behave similarly at an angular deviation of the crystal from the Bragg position only when this deviation satisfies the condition $|y_c| < Dt$. With an increase in strain, the angular range of total reflection increases, and the size of the crystal region where trajectories are rotated decreases.

Thus, formula (6) describes all observed features of beam switching in the reflection direction: the linear increase in the integrated intensity at low strains and saturation at high strains. The latter process occurs only when the angular range of incident radiation is limited in the experiment. Since only one Bloch wave is excited, the interference oscillations in both the thickness and angular dependences of the reflection disappear.

It is also useful to discuss the qualitative description of the switching effect using the concepts of dispersion surface [4, 5] and energy-flux vector in each Bloch wave $\mathbf{S} = \mathbf{s}_0(E''_0)^2 + \mathbf{s}_h(E''_h)^2$, where $\mathbf{s}_0$ and $\mathbf{s}_h$ are the unit vectors in the directions of the transmitted and diffracted beams. According to the Kato theorem [6], the energy flux is always directed perpendicularly to the local dispersion surface at the excitation point. In turn, the excitation point on the input surface is determined by the deviation of the wave vector of the incident wave from the exact Bragg position for a local region in the crystal, with allowance for strains. The above-considered case is illustrated in Fig. 1.

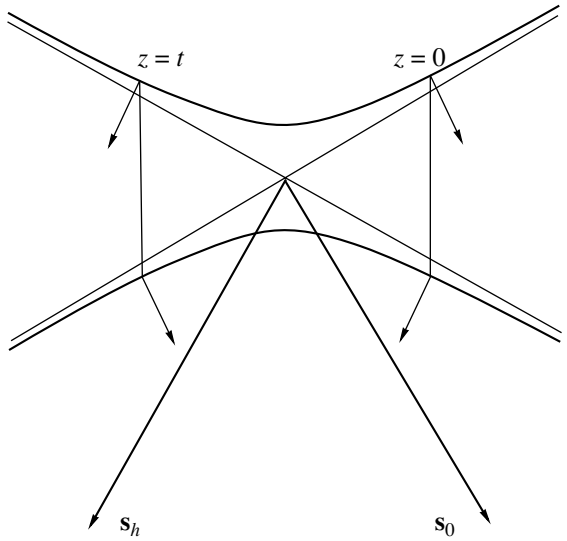

Fig. 1. Schematic diagram of the dispersion surface with the directions of the energy-flux vectors along the normal to the surface at the excitation point.

Let the crystal be first located in the exact Bragg position. Then, owing to the strain on the input surface ($z = 0$), the excitation point is on the right. In this case, the energy flux direction (normal to the dispersion surface) for the upper zone, corresponding to the second (weakly absorbed) wave, almost coincides with that of the incident wave. Naturally, specifically this region is most strongly excited, whereas the lower zone is almost unexcited. For a strain slowly varying with an increase in z, as was noted above, the waves corresponding to different regions are almost independent; therefore, it is sufficient to consider each of them separately. If the lower zone is unexcited, there is no point in analyzing its behavior. Concerning the upper zone, during transmission of radiation into the crystal bulk, the local Bragg condition slowly changes, as a result of which the excitation point moves along the dispersion surface from the right to the left. Finally, on the output surface ($z = t$), the excitation point moves to the left region, where the energy flux direction coincides with that of the reflected wave. At the output of the crystal, the energy flux should be expanded in projections on the directions of the incident and reflected waves. Obviously, the expansion coefficient for the reflected wave will greatly exceed that for the incident wave. If the crystal is rotated by a certain angle, the excitation points on the input and output surfaces are displaced; however, this displacement does not change the general pattern until the crystal rotation extracts the initial and final excitation points from the crystal sides.

An even simpler interpretation of the switching effect follows from consideration of ray trajectories in a crystal, as was discussed above. In [1], it was shown that the energy flux direction coincides with the tangent to the trajectory. For a weakly absorbed wave, the trajectories are first almost parallel to the incident beam. Then, they are bent toward the reflected beam at the depth where the dynamical diffraction condition is satisfied. At the output of the crystal, they are almost parallel to the reflected beam. For the strongly absorbed wave, everything is vice versa; however, the amplitude of such a wave is small.

Obviously, if a crystal is heated from the opposite side, the entire analysis holds true. The only difference is that the beam will be reflected via the strongly absorbed wave and, therefore, will be more strongly absorbed at a low strain. A similar effect will occur in the case of crystal deformation by ultrasound forming an appropriate strain, for example, when a piezoelectric quartz crystal is used.

NUMERICAL SIMULATION

The trajectory method not only makes it possible to qualitatively describe the total reflection phenomenon but also provides a relatively simple technique of numerical simulation of the most complicated case of spherical wave diffraction in a deformed crystal at any distances from the source to the crystal. In this case, a significant gain in computation time is obtained in comparison with not only the direct solution of the Takagi equations [7] but also the Wentzel–Kramers–Brillouin approximation [8, 9]. Numerical calculations were performed using the program described in [1].

The calculations were performed for an example of a Si crystal with the thickness $t = 500$ μm for the 220 diffraction of MoK_α radiation ($E = 17.48$ keV). Two cases were considered: large (40 m) and small (50 cm) distances from the point source to the crystal. The diffraction parameters were calculated using the program reported in [10] and found to be $\mu_0 = K\chi_{i0} = 1.435$ cm^{-1} and $K\chi_h = (-169.9 + 1.39i)$ cm^{-1}. The Bragg angle is $\theta_B = 10.64°$.

The results of the calculation for the first case are shown in Fig. 2. The intensity of the reflected wave is shown relative to the intensity of the incident wave before the crystal. The trajectories are considered in a finite region of the wavefront with a width of 1.6384 mm; such consideration is equivalent to the situation where a slit with such a width is installed in the beam path before the crystal. Figure 2a shows the spatial structure of the reflected beam directly behind the crystal in the case of absence of strain. The spherical-wave focusing thickness [1] for a distance of 40 m from the source is 1.144 mm, a value that exceeds the crystal thickness by a factor of more than 2. Therefore, the trajectories do not cross each other; however, they slightly and nonuniformly change their direction. Accordingly, the spatial structure of the reflected beam shows extinction beatings, as in the angular dependence of the plane wave reflection; i.e., the oscillations are caused by the interference of two Bloch waves with a changing phase difference between them. Nevertheless, for the first

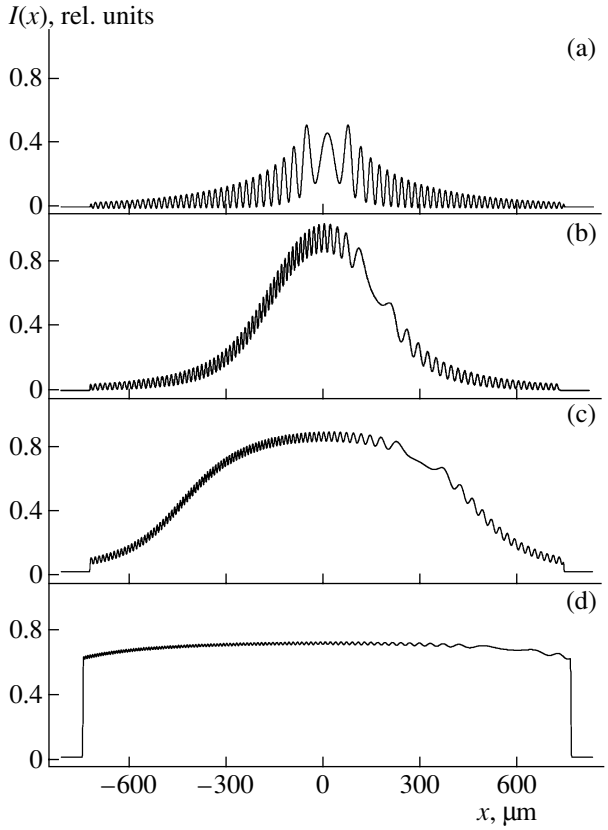

Fig. 2. Spatial structure of the reflected beam in the case of diffraction of a spherical wave from a point source located at a distance of 40 m from a crystal (a) without bending and (b–d) with atomic-plane bending characterized by the radius R = (b) 36, (c) 18, and (d) 9 m.

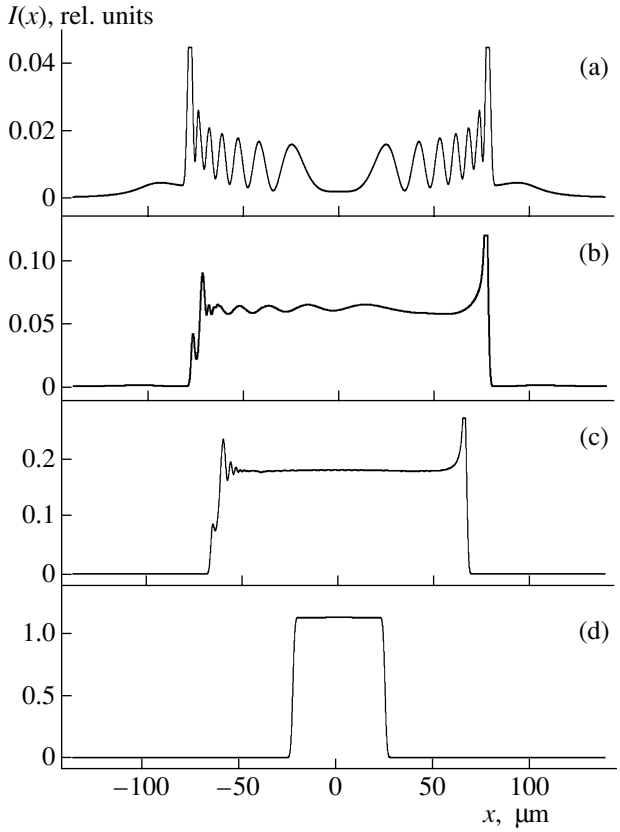

Fig. 3. Spatial structure of the reflected beam in the case of diffraction of a spherical wave from a point source located at a distance of 50 cm from a crystal (a) without bending and (b–d) with atomic-plane bending characterized by the radius R = (b) 18, (c) 6, and (d) 2 m.

wave, the reflected beam width slightly exceeds the slit width (trajectories diverge), whereas for the second wave, vice versa, the reflected beam width is somewhat smaller (trajectories converge). Correspondingly, oscillations can be seen in a narrower region, where both waves exist.

At the radius of strain curvature R = 36 m, reflection increases in the central part of the wavefront, whereas the oscillation amplitude decreases (Fig. 2b). Since it is the weakly absorbed Bloch wave that reflects, owing to the Borrmann effect, the reflectance is higher than in the case of normal absorption with the factor $\exp(-\mu_0 t/\cos\theta_B)$ = 0.482. The asymmetry of oscillations is related to the finite distance to the spherical-wave source. For the purely angular dependence, the pattern is similar but symmetric [11]. It can clearly be seen that the intensity of the first Bloch wave (at the edges) is almost zero, whereas the oscillation amplitude is still fairly large. This is a general property of interference effects.

In Fig. 2c, the radius of curvature is R = 18 m. Now, the wider part of the wavefront maximally reflects, although the maximum value itself is smaller. The reason for this fact is that the dynamic reflection region in the crystal is reduced and the absorption losses increase at the expense of the parts where reflection is absent. In Fig. 2d, the radius R = 9 m. Almost the entire beam maximally reflects; however, the maximum value became smaller. In addition, since only the second Bloch wave reflects, the reflected beam is somewhat smaller in width than the incident one. With a further decrease in the radius of strain curvature, almost nothing occurs, except for the fact that the oscillation amplitude tends toward zero, while the maximum value tends toward 0.482. At the same time, if there were no slit, the width of the maximum reflection front would continue to increase. Thus, the bending-deformed crystal is an extremely good reflector in the case of Laue diffraction.

Figure 3 shows the calculation results for the case where the spherical-wave source is located at a small distance (50 cm) from the crystal. In this case, the focusing thickness is 14.3 μm, i.e., much smaller than the crystal thickness. This situation is closer to the well-known case of the Kato diffraction of a spherical wave [4, 5], where the source is assumed to be placed on the input crystal surface. In this case, the source formally exposes the entire input surface, although the area on the surface where rays are under the dynamical diffraction conditions is small. Its size can easily be estimated

as the size of the region in Fig. 2, diminished by a factor of 80 (i.e., 15 μm).

In the calculation, we considered the trajectories in the region with a size of 104.8 μm; i.e., it can be assumed that a slit with such a width is located before the crystal. In most cases, this assumption absolutely does not affect the results. Figure 3a shows the well-known intensity distribution for an unstrained crystal. Strong reflection occurs in the crystal in the region referred to as the Borrmann fan [4], which is limited by the peaks arising during rotation of trajectories and their crowding (caustics). As was shown in [1], the trajectory method slightly overestimates the height of these peaks; therefore, the peak height in the figure was corrected to smaller sizes. In the middle of the beam, the average intensity is lower than the incident intensity by a factor of 100. One of the reasons for such a decrease is that the region 15 μm in size is extended (nonuniformly) to 160 μm.

At the radius of curvature $R = 18$ m, as in the case of a large distance, strain enhances reflection and reduces oscillations; i.e., the degree of reflection via the second (weakly absorbed) Bloch wave increases (Fig. 3b). The beam width decreases because trajectories for this wave in an unstrained crystal cross each other (are focused) and then diverge again. The strain as if corrects the normal run of trajectories, as a result of which the focusing depth increases, and the focusing becomes less sharp. Accordingly, trajectories fail to diverge as strongly as in the absence of strain.

In Fig. 3c, the radius of strain curvature is $R = 6$ m. As follows from the calculation, the above-described tendencies are enhanced; i.e., reflection increases, oscillations disappear, and the beam narrows. The presence of caustics means that the slit does not affect the beam size. In Fig. 3d, the radius of curvature is $R = 2$ m. Only in this case of very high strain is reflection homogeneous throughout the beam width, whereas the beam size is proportional to the entrance slit width. This fact indicates that strain in the initial stage "straightens" all the considered trajectories in the second wave along the incident beam direction and then bends them toward the reflection direction. However, different rays fall in the dynamical reflection region at different depths in the crystal. Therefore, the reflected beam is effectively narrowed. At a higher strain, it slightly increases in size again, and then saturation occurs. However, it is difficult to obtain such high strains in practice.

Thus, the trajectory method is an effective tool for describing the total reflection phenomenon in the case of Laue diffraction in crystals with bending deformation. This method makes it possible to describe not only qualitatively but also quantitatively all fine features of the noted effect and, at the same time, sharply reduce the computation time. Although all calculations were performed only for case of parabolic plane bending, similar results can be obtained in the case of ultrasound excitation of crystals, where a half of the ultrasonic wavelength corresponds to the crystal thickness.

ACKNOWLEDGMENTS

This study was supported by the Russian Foundation for Basic Research, project nos. 05-02-16702, 06-02-08117-ofi, 07-02-00067-a, and NSh-6869.2006.2.

REFERENCES

1. V. G. Kohn, Kristallografiya **52** (4), 625 (2007) [Crystallogr. Rep. **52**, 598 (2007)].
2. A. P. Mkrtchan, M. A. Navasardyan, and V. K. Mirzoyan, Pis'ma Zh. Tekh. Fiz. **8**, 677 (1982) [Sov. Tech. Phys. Lett. **8**, 294 (1982)].
3. M. A. Navasardyan, J. Appl. Crystallogr. **34**, 763 (2001).
4. Z. G. Pinsker, *X-ray Crystal Optics* (Nauka, Moscow, 1982) [in Russian].
5. A. Autier, *Dynamical Theory of X-ray Diffraction* (Oxford Univ. Press, New York, 2001).
6. N. Kato, Acta. Crystallogr. **11**, 885 (1958).
7. R. G. Gabrielyan and A. A. Aslanyan, Izv. Akad. Nauk Arm. SSR, Ser. Fiz. **21**, 337 (1986).
8. A. R. Mkrtchan, R. G. Gabrielyan, A. G. Unanyan, and F. G. Beglaryan, Izv. Akad. Nauk Arm. SSR, Ser. Fiz. **21**, 313 (1986).
9. E. A. Tikhonova, Metallofizika **3**, 18 (1981).
10. V. G. Kohn, Kristallografiya **51** (6), 1001 (2006).
11. V. G. Kohn, Phys. Status Solidi B **231**, 132 (2002).

Translated by Yu. Sin'kov